

# Carbon Nanoparticles on Carbon Fabric for Flexible and High-Performance Field Emitters

Longyan Yuan, Yuting Tao, Jian Chen, Junjie Dai, Ting Song, Mingyue Ruan, Zongwei Ma, Li Gong, Kang Liu, Xianghui Zhang, Xuejiao Hu, Jun Zhou,\* and Zhong Lin Wang\*

Carbon nanoparticles (CNPs) are grown on flexible carbon fabric via a simple and low-cost flame synthesis process. The entire structure of the carbon fabric substrate retains its high flexibility after the growth of CNPs and can even be rolled-up and twisted to a large degree without affecting the electric characteristics. No appreciable changes in the conductance can be observed under different bending curvatures after hundreds of bending cycles. The thermal conductivity of the carbon fabric with CNPs is about  $2.34 \text{ W m}^{-1} \text{ K}^{-1}$ , about one order of magnitude higher than that of most polymer substrates. The field emitter fabricated using the structure has a low threshold electric field of around  $2.8 \text{ V } \mu\text{m}^{-1}$ , and a high field emission current density of  $108 \text{ mA cm}^{-2}$ , which is about two to four orders of magnitude higher than that of most polymer substrate-based flexible CNT field emitters. These results indicate that CNPs on carbon fabric have potential applications in flexible electronics devices and displays.

## 1. Introduction

Flexible electronics have attracted extensive attention in the last decade because of their high flexibility, foldability and conformability. Replacing the rigid substrates by ones that are flexible or stretchable is likely to have applications including, but not

limited to, paper displays, electronic textiles, distributed sensors, wearable electronics and large area circuits on curved objects.<sup>[1–3]</sup> Flexible displays have been proven viable by electrophoretic displays and curved liquid crystal displays (LCDs) on plastic that have reached the market. Besides the mentioned applications for flexible displays, field emission displays (FEDs) on flexible substrates may realize roll-up displays that are likely to impact everyone's daily life.<sup>[4,5]</sup>

Among the materials for FEDs, low-dimensional nanostructures have received increasing attention due to their small tip radius and high aspect ratio, which are ideal for field emission. Carbon nanotubes (CNTs) on polymer substrates as field emitters are an attractive choice for flexible FEDs, which could integrate the

merits of CNTs with flexible, low-cost polymers.<sup>[6–9]</sup> Despite their good electron emission properties, problems arising from the polymer substrates may hinder their potential applications, such as the poor interlayer bonding between CNTs and the polymer substrate, the low thermal conductivity and the low thermal degeneration temperature of the substrate. Moreover, CNTs are mostly grown by chemical vapor deposition (CVD) at high temperature, and even a raw sample needs purification and/or the transfer of CNTs onto a conducting substrate for field emission measurements, which are costly and fairly lengthy. Thus, an industrial-scale fabrication method for flexible field emission emitters is greatly desired. Recently, we grew tungsten oxide nanowire arrays on a flexible carbon fabric, which demonstrated good field emission properties<sup>[10]</sup> and sheds light on the fabrication of high quality flexible FEDs.

In this paper, we report a simple and low-cost flame synthesis process to fabricate carbon nanoparticles (CNPs) on carbon fabric to enhance their field emission performance. This procedure can easily be accommodated by process-line-scale manufacturing for to yield large area products. The processed carbon fabric possesses novel properties, such as high flexibility, excellent electrical and thermal conductivity, high aspect ratio, and thermal and chemical stability. The emitter has a low threshold electric field of around  $2.8 \text{ MV m}^{-1}$  and a high field emission current density of around  $108 \text{ mA cm}^{-2}$ , demonstrating its great potential for flexible FED applications.

Dr. L. Yuan,<sup>[†]</sup> J. J. Dai, T. Song, M. Y. Ruan, Z. W. Ma, X. H. Zhang,

Prof. J. Zhou, Prof. Z. L. Wang

Wuhan National Laboratory for Optoelectronics (WNLO)

and College of Optoelectronic Science and Engineering

Huazhong University of Science and Technology (HUST)

Wuhan, 430074, P. R. China

E-mail: jun.zhou@mail.hust.edu.cn

Y. Tao,<sup>[†]</sup> Prof. J. Chen, L. Gong

Instrumental Analysis & Research Center

Sun Yat-sen University

Guangzhou, 510275, P. R. China

K. Liu, Prof. X. J. Hu

School of Power and Mechanical Engineering

Wuhan University

Wuhan, 430072, P. R. China

Prof. Z. L. Wang

School of Materials Science and Engineering

Georgia Institute of Technology

Atlanta, Georgia 30332-0245, USA

E-mail: zhong.wang@mse.gatech.edu

[†] L.Y. and Y.T. contributed equally to this work.

DOI: 10.1002/adfm.201100172

## 2. Results and Discussion

CNPs were grown on highly conductive, highly flexible and robust carbon fabric through a simple and low-cost flame synthesis process. The experimental settings are shown in **Figure 1a**. The structure of the CNPs has been studied by electron microscopy. **Figure 1b** shows optical images of the carbon fabric after growing CNPs on its surface. The flatness and uniform black color at the center part of the carbon fabric demonstrates the uniformity of the synthetic CNPs. In addition, the carbon fabric retains its high flexibility after the growth of CNPs and can even be bent into a circle (left inset of **Figure 1b**) or spiral (right inset of **Figure 1b**) without destroying the structural integrity of the CNPs. **Figures 1c** and **d** show low-magnification scanning electron microscopy (SEM) images of the carbon fabric before and after the growth of CNPs, respectively. The diameters of the original carbon fibers are about 10  $\mu\text{m}$ . After the growth of CNPs, the surfaces of the carbon fibers are fully covered by a brushy and porous nanostructure and the diameters of the fibers has increases to 30–50  $\mu\text{m}$ , which can be seen in **Figure 1e**. The detailed microstructures of the CNPs were characterized by using transmission electron microscopy (TEM). **Figure 1f** shows a typical low-magnification TEM image of the as-growth CNPs, indicating that the CNPs

have a dendrite-like morphology and are composed of nanoparticle network-like structures, which are curved and twisted with each other. **Figure 1g** shows a high resolution TEM (HRTEM) image of the CNPs. It revealed that the CNPs are composed of many curved carbon lamellae, some of which are concentric, forming onion-like structures. The onion-like CNPs stacked with several curved graphene layers has a graphitic structure.

The Raman spectrum from the CNPs is illustrated in **Figure 2**. It can be seen that the G peak at 1 608  $\text{cm}^{-1}$  and D peak at 1 352  $\text{cm}^{-1}$  have the highest intensity in the spectrum. The G vibration mode is usually used to identify the graphite ordering of carbon materials, which involves the in-plane bond-stretching motion of pairs of C  $\text{sp}^2$  bonding, while the D peak is only active in the presence of disorder.<sup>[11,12]</sup> The results indicate that the CNPs grown on carbon fabric possess a structure analogous to that of graphite with some degree of disordering. The in-plane crystallite size  $L_a$  can be obtained from the equation,<sup>[13]</sup>

$$L_a(\text{nm}) = (2.4 \times 10^{-10})\lambda^4 \left( \frac{I_D}{I_G} \right)^{-1} \quad (1)$$

where  $I_D$  and  $I_G$  are the intensity of the D and G peaks, respectively, and  $\lambda$  is the wavelength of the laser. The calculated crystal size is approximately 6.7 nm, which coincides with the result from TEM measurements. Other peaks at about 2 676, 2 930 and 3 182  $\text{cm}^{-1}$  can be designated 2D, D + G and 2D' modes, respectively, which are the doubling or sum frequency of G, D and D'.

We also grew CNPs on carbon fabric without Ni catalyst. In our experiments, the synthetic CNPs on carbon fabric with or without sputtered Ni exhibited no obvious difference in microstructure, as observed by SEM and TEM, besides the CNPs showing a stronger adhesion to the Ni-coated carbon fabric. In addition, the size of CNPs remained nearly unchanged when the growth time varied from 30 s to 5 min at a certain height above the burner, as demonstrated by SEM, TEM and Raman spectrum measurement. This may enable a good 'manufacturing' process with good yield of similar fabric field emitters. It has been reported that the formation of CNPs is initiated by pyrolysis of the hydrocarbon at moderate temperature of about 800  $^{\circ}\text{C}$ .<sup>[14]</sup> The building blocks in CNPs formation were intermediate radicals such as  $\text{C}_2\text{H}$  or  $\text{C}_4\text{H}_3$ , which agglomerated to polycyclic aromatic hydrocarbons (PAHs) and fullerenes through cyclization reactions, followed by dehydrogenation.<sup>[15,16]</sup> Ethanol may undergo pyrolysis through the following two reactions,<sup>[17]</sup>

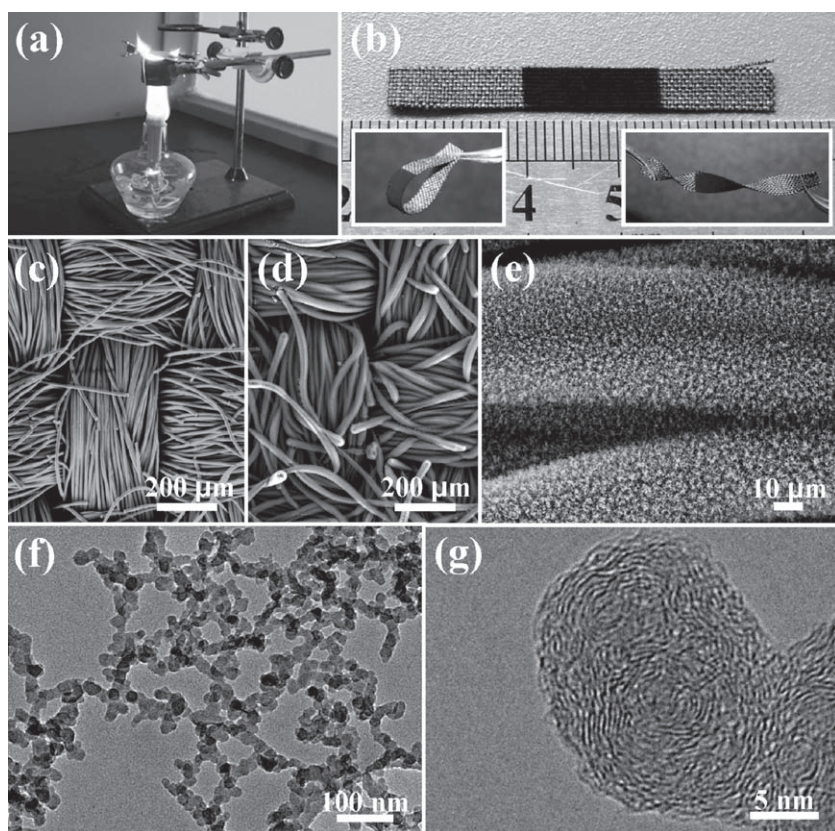
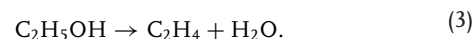
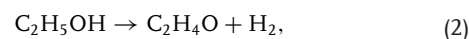


**Figure 1.** a) Optical photograph of the experimental setup. The carbon fabric substrate is placed in the flame core about 5.5 cm above the wick. b) Optical photographs of CNPs grown on carbon fabric. The black color of the centre area of the carbon fabric indicates the presence of CNPs. The left-bottom and right-bottom insets show the flexibility of carbon fabric with CNPs, which can be bent into a circle or spiral. c, d) SEM images of carbon fabrics before and after the growth of CNPs, respectively. e) A magnified SEM image of the CNPs on carbon fabric. f, g) Low- and high-resolution TEM images of CNPs, respectively.

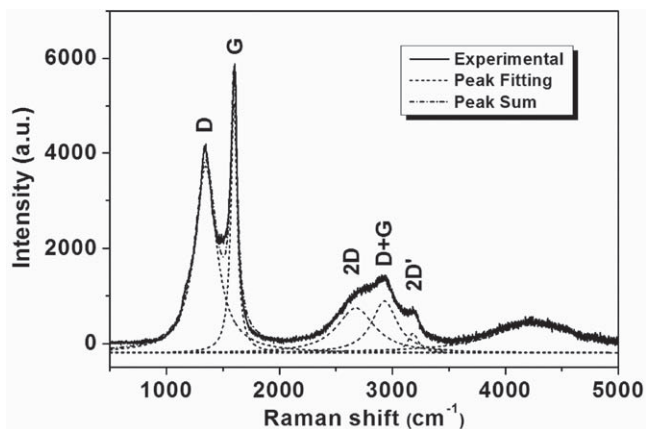


**Figure 2.** Room temperature Raman spectrum of CNPs. The solid line is experimental data, while the short dot lines are fitting curves.

The decomposed  $C_2H_4$  could convert into  $C_2H_2$  following the same reaction sequence as  $C_2H_2$  forming PAHs, while  $C_2H_4O$  plays an important role in producing a carbon nanostructure with curved and stacked graphene layers. There is a critical balance between the reactions (2) and (3) to the formation of onion-like carbon nanostructure. By covering the surface of the smaller PAHs with curved graphene layers through an aerosol process, the PAHs grow larger.<sup>[18–20]</sup> Increasing the pyrolysis temperature therefore accounts for the greater degree of crystallization or graphitization of CNPs, such as carbon onions formed at 1 650 °C.<sup>[18,21,22]</sup> In our experiment, the carbon onions are surrounded by randomly distributed graphene layers due to the relatively low temperature of about 790 to 830 °C for the ethanol flame used.

In order to probe the feasibility of the material for flexible electronic devices, the effect of curvature on the electrical properties of the carbon fabric substrate with CNPs was measured by the following method. A carbon fabric substrate with CNPs on it was placed on two X–Y–Z mechanical stages with a fine moving step of 2  $\mu\text{m}$ . Each end of the substrate was fixed on one stage by copper foil electrode (see the Supporting Information, Figure S1). The bending curvature of the carbon fabric substrate was precisely controlled by adjusting the stages. As can be seen in the left-bottom inset of Figure 3, the linear behavior of the current versus voltage ( $I$ – $V$ ) curve shows good Ohmic contact between the Cu foil and the carbon fabric. The total resistance was calculated to be about 3.0  $\Omega$  (0.5 cm  $\times$  1.5 cm), including the contact resistance between Cu and carbon fabric. The conductance stability of the carbon fabric with CNPs on it under different bending curvature was studied. In this measurement, the applied voltage was fixed at +0.5 V and the current was continuously recorded. We checked the currents under five different bending conditions (each bending condition was maintained for 60 s),

which are shown in the upper insets, labeled as I, II, III, IV and V. The current is observed to have no apparent change, revealing that the conductance of the carbon fabric substrate is hardly affected by bending stress. Measurement of the carbon fabric substrate's folding endurance was conducted by bending the substrate from stage I to V then releasing to stage I (one cycle). Even after 100 cycles of bending, the conductance of the substrate remained unchanged (right-bottom inset of Figure 3). These results indicate the high flexibility and stability of the carbon fabric substrate with CNPs on it.

The thermal conductivity of the carbon fabric with CNPs on it was measured by a transient electrothermal (TET) method. The inset of Figure 4 shows the measurement settings. Two copper foils attaching on a slide glass were used as electrodes to measure the voltage over the carbon fabric covered them. Electrical voltage was forced on the carbon fabric through two copper wires pressing on the CNPs, through which the current flowed and was heated. The sample was subjected to a step-rise electrical power at room temperature  $T_0$ . The temperature of the copper electrodes was supposed to be constant since a small current flowing through them. At  $t \geq 0$ , the temperature change was obtained by measuring the voltage variation, shown in Figure 4. The normalized temperature increase  $T^*(t) = [T(t) - T_0]/[T(t \rightarrow \infty) - T_0]$  can be calculated as,<sup>[23]</sup>

$$T^* = \frac{96}{\pi^4} \sum_{m=1}^{\infty} \frac{1 - \exp[-(2m-1)^2 \pi^2 \alpha t / L^2]}{(2m-1)^4} \quad (4)$$

where  $\alpha$  is thermal diffusivity,  $t$  is time and  $L$  is the length of the sample. The above result is valid without considering radiation.<sup>[24]</sup> The fitted data of the temperature rise with equation 4 are also plotted in Figure 4. The thermal diffusivity value is found to be  $1.27 \times 10^{-6} \text{ m}^2 \text{ s}^{-1}$ . The thermal conductivity of the sample is roughly calculated to be 2.34  $\text{W m}^{-1} \text{ K}^{-1}$ , using the density and specific heat of graphite, about one order of magnitude higher than that of the polyethylene terephthalate (PET) substrate (0.15–0.4  $\text{W m}^{-1} \text{ K}^{-1}$ ).<sup>[7]</sup>

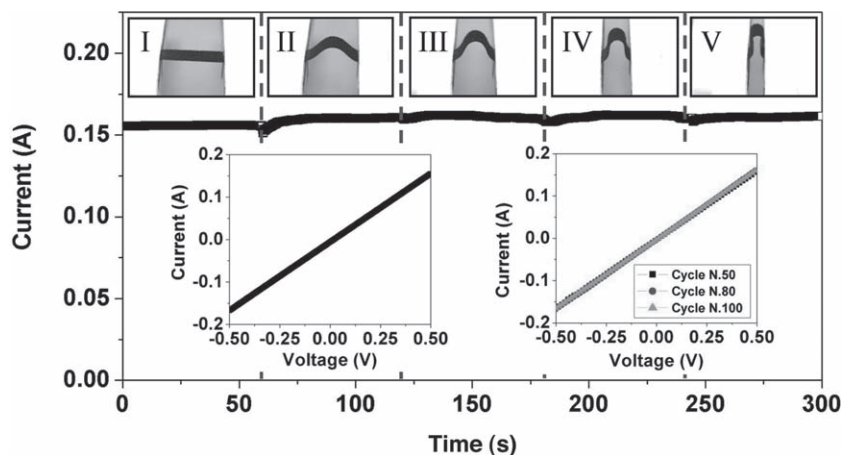


**Figure 3.**  $I$ – $T$  curve of carbon fabric strip bent with different curvatures under a constant voltage. The upper insets labeled as I, II, III, IV, V demonstrate the five bending stages, each of which was maintained for 60 s. The bottom left inset shows the  $I$ – $V$  curve of carbon fabric with CNPs without bending. The bottom right inset records the  $I$ – $V$  curve of carbon fabric after 50, 80 and 100 cycles of bending.



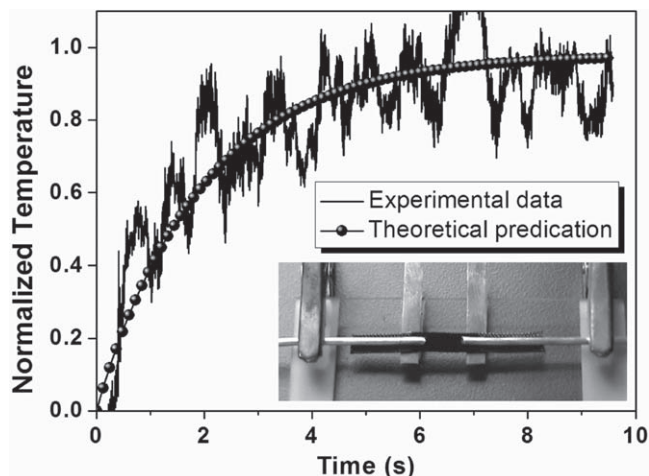


**Figure 4.** Normalized temperature rise versus time for carbon fabric after the growth of CNPs. The inset illustrates the measurement settings by a transient electrothermal method.

A field emission study of the CNPs on carbon fabric substrate was carried out at room temperature by using a probe technique.<sup>[25]</sup> The vacuum gap between the anode and CNPs was approximately 420  $\mu\text{m}$ . The volume of CNPs grown on carbon fabric affected the morphology of the electron emitters, from is crucial for electron emission. The bare carbon fabric exhibited poor field emission,<sup>[10]</sup> while excessive CNPs on the carbon fabric would form a CNPs film, which may show inferior electron emission property due to an electrostatic screening effect.<sup>[26,27]</sup> This problem can be solved simply by controlling the CNP growth time. A typical plot of emission current density versus electric field ( $J$ - $E$ ) from CNPs grown for 1 min is shown in **Figure 5a**. The field emission turn-on field ( $E_{\text{to}}$ ) and threshold field  $E_{\text{th}}$ , defined as the macroscopic field required to produce a current density of  $10 \mu\text{A cm}^{-2}$  and  $10 \text{mA cm}^{-2}$  are about 1.33 and 2.8  $\text{MV m}^{-1}$ , respectively. The highest electron emission current density, of about  $108 \text{mA cm}^{-2}$  at  $7.3 \text{MV m}^{-1}$ , can be achieved after conditioning (see the Supporting Information, Figure S2). To the best of our knowledge, the obtained field emission current density is about two to four orders of magnitude larger than that of most polymer substrate-based flexible CNT field emitters.<sup>[4,6-10]</sup>

The field emission  $J$ - $E$  characteristics were analyzed using the Fowler-Nordheim (FN) equation,<sup>[28]</sup>

$$\ln\left(\frac{J}{E^2}\right) = \ln\left(\frac{A\beta^2}{\phi}\right) - \frac{B\phi^{3/2}}{\beta E} \quad (5)$$

where  $E$  is the applied electric field,  $A = 1.54 \times 10^{-6} \text{A eV V}^{-2}$ ,  $B = 6.83 \times 10^3 \text{eV}^{-3/2} \text{V } \mu\text{m}^{-1}$ ,  $\phi$  is the work function of the emitter material and  $\beta$  is the field enhanced factor. The corresponding  $F$ - $N$  curve, plotted as  $\ln(J/E^2)$  versus  $1/E$ , is shown in the inset of **Figure 5a**. The linear relationship between  $\ln(J/E^2)$  and  $1/E$  demonstrates that the CNPs grown on carbon fabric follows the field emission behavior well. By taking 4.0 eV as

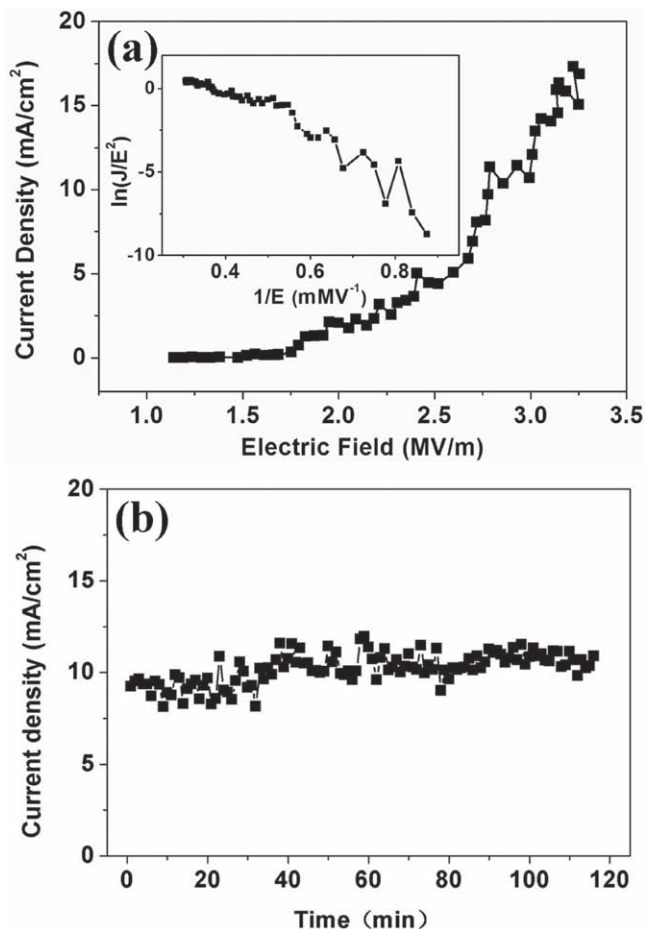


**Figure 5.** a) Field emission current density versus electric field of CNPs on carbon fabric. The left inset is the corresponding  $F$ - $N$  curve. b) The field emission stability of CNPs on carbon fabric over time.

the work function value for the CNPs,<sup>[29]</sup> the field enhanced factor  $\beta$  can be calculated to be  $4.2 \times 10^3$ . The emission stability test of CNPs was performed by recording the emission current every minute under an emission current of approximately  $10 \text{mA cm}^{-2}$  for 120 min. As shown in **Figure 5b**, no obvious emission degradation is observed and the fluctuation is about 10%.

The good field emission characteristics of CNPs on carbon fabric may be attributed to the following factors: firstly, the low work function of the CNPs could reduce the height of potential barrier, leading to electrons emitting from it more easily; secondly, the ultrafine onion-like structure of CNPs has a high aspect ratio, and the localized electrical field on the outer surface of the CNP is greatly enhanced, which also reduces the threshold field; thirdly, the low resistance of the carbon fabric substrate guarantees an abundant electron source, which further enlarges the emission current; and, finally, the excellent thermal conductivity and the thermal stability of the carbon fabric substrate benefits the high emission current. All of the above factors result in the high emission current density and low threshold electrical field of CNPs grown on flexible carbon fabric.

### 3. Conclusions

In summary, CNPs were grown on flexible carbon fabric via a low-cost flame synthesis process. This method can easily scaled-up to process-line-scale manufacture yielding large-scale terminal products. The electrical resistance of the CNPs with carbon fabric is around  $3.0 \Omega$  and the thermal conductivity  $2.34 \text{ W m}^{-1} \text{ K}^{-1}$ . CNPs on carbon fabric exhibited good field emission characteristics, such as a low threshold electrical field of around  $2.8 \text{ MV m}^{-1}$ , a high emission current density of around  $108 \text{ mA cm}^{-2}$  and long-term field emission stability. This was spurred an intense drive to finally realize the long-held dream of lightweight and flexible displays. These results indicate that CNPs on carbon fabric have potential applications in flexible electronic devices including rollable field emission displays, X-ray radiotherapy, microwave amplifiers and more.

### 4. Experimental Section

**CNP Synthesis:** A common alcohol burner in a room without apparent cross-ventilation was used to produce CNPs. About 10 to 15 min after the ignition of the wick, a steady ethanol flame was obtained with a total flame height of 8.5 cm. A carbon fabric strip coated with 10 nm sputtered Ni was mounted in the flame core 5.5 cm above the wick. The temperature of the surface of carbon fabric was in the range of 790 to 830 °C which was measured through a thermoelectric couple test. The growth process lasted for 30 s to 5 min, after which the carbon fabric was taken out from the flame. The color of the surface exposed to flame turned from grey to black, indicating the formation of CNPs. In fact, CNPs could also be grown on different common substrates in our experiment, including Si wafers, ceramic slices and quartz, whether the substrates were coated with Ni or not. The synthetic CNPs on carbon fabric with or without sputtered Ni exhibited no obvious difference in microstructure, as observed by SEM and TEM, besides the CNPs showing a stronger adhesion to Ni-coated carbon fabric.

**CNP Characterization:** The morphologies of the prepared products were characterized with high-resolution field emission scanning electron microscopy (SEM: FEI Sirion 200), and field emission transmission electron microscopy (TEM: JEM-2010HR). Raman scatter measurements were performed on a Renishaw-inVia Raman spectrometer at room temperature using the 514.5 nm line of an Ar<sup>+</sup> laser.

**Conductance Measurement:** Conductance measurements on the carbon fabric under different curvatures after the CNPs growth were carried out on a homemade probe table. The carbon fabric was cut into strips  $5 \text{ cm} \times 0.5 \text{ cm}$  in dimension, and then placed on two X–Y–Z mechanical stages with a fine moving step of 2  $\mu\text{m}$ ; each end of the substrate was fixed on one stage by copper foil electrode. The I–V curves under different curvatures were measured using an electrochemical station (CHI660D). During the measurement, the voltage was fixed at +0.5V.

**Field-Emission Measurement:** A field emission study of the CNPs on carbon fabric substrate was carried out in a vacuum chamber at a pressure of  $1.0 \times 10^{-7}$  torr at room temperature using a probe technique. A stainless-steel probe with a diameter (2R) of 0.35 mm was used as the anode and the CNPs on carbon fabric substrate as cathode. The vacuum gap (d) between anode and the grounded cathode was maintained at a certain distance (approximately 420  $\mu\text{m}$ ) during the entire measurement.

### Supporting Information

Supporting Information is available from the Wiley Online Library or from the author.

### Acknowledgements

This work was financially supported by the National Natural Science Foundation of China (51002056, 51072236), the Program for New Century Excellent Talents in University (NCET-10-0397), a Foundation for the Author of National Excellent Doctoral Dissertation of PR China (201035) and the startup fund from HUST (01-24-182021, 01-24-187051). The authors thank Professor Juncong She from Sun Yat-sen University for his help. The authors thank the Analysis and Testing Center of Huazhong University of Science and Technology for support.

Received: January 21, 2011

Published online:

- [1] K. Takei, T. Takahashi, J. C. Ho, H. Ko, A. G. Gillies, P. W. Leu, R. S. Fearing, A. Javey, *Nat. Mater.* **2010**, *9*, 821.
- [2] K. Nomura, H. Ohta, A. Takagi, T. Kamiya, M. Hirano, H. Hosono, *Nature* **2004**, *432*, 488.
- [3] A. Dodabalapur, *Mater. Today* **2006**, *9*, 24.
- [4] H. S. Sim, S. P. Lau, H. Y. Yang, L. K. Ang, M. Tanemura, K. Yamaguchi, *Appl. Phys. Lett.* **2007**, *90*, 143103.
- [5] Y. G. Sun, J. A. Rogers, *Adv. Mater.* **2007**, *19*, 1897.
- [6] O. J. Lee, K. H. Lee, *Appl. Phys. Lett.* **2003**, *82*, 3770.
- [7] C. Y. Wang, T. H. Chen, S. C. Chang, T. S. Chin, S. Y. Cheng, *Appl. Phys. Lett.* **2007**, *90*, 103111.
- [8] P. Ghosh, M. Z. Yusop, S. Satoh, M. Subramanian, A. Hayashi, Y. Hayashi, M. Tanemura, *J. Am. Chem. Soc.* **2010**, *132*, 4034.
- [9] Y. J. Jung, S. Kar, S. Talapatra, C. Soldano, G. Viswanathan, X. S. Li, Z. L. Yao, F. S. Ou, A. Avadhanula, R. Vajtai, S. Curran, O. Nalamsu, P. M. Ajayan, *Nano Lett.* **2006**, *6*, 413.
- [10] X. H. Zhang, L. Gong, K. Liu, Y. Z. Cao, X. Xiao, W. M. Sun, X. J. Hu, Y. H. Gao, J. Chen, J. Zhou, Z. L. Wang, *Adv. Mater.* **2010**, *22*, 5292.
- [11] M. A. Pimenta, G. Dresselhaus, M. S. Dresselhaus, L. G. Cancado, A. Jorio, R. Saito, *Phys. Chem. Chem. Phys.* **2007**, *9*, 1276.
- [12] A. C. Ferrari, J. Robertson, *Phys. Rev. B* **2000**, *61*, 14095.
- [13] L. G. Cancado, K. Takai, T. Enoki, M. Endo, Y. A. Kim, H. Mizusaki, A. Jorio, L. N. Coelho, R. Magalhaes-Paniago, M. A. Pimenta, *Appl. Phys. Lett.* **2006**, *88*, 163106.
- [14] M. Choi, I. S. Altman, Y. J. Kim, P. V. Pikhitsa, S. Lee, G. S. Park, T. Jeong, J. B. Yoo, *Adv. Mater.* **2004**, *16*, 1721.
- [15] H. Richter, J. B. Howard, *Prog. Energy Combust. Sci.* **2000**, *26*, 565.
- [16] V. J. Hall-Roberts, A. N. Hayhurst, D. E. Knight, S. G. Taylor, *Combust. Flame* **2000**, *120*, 578.
- [17] T. S. Norton, F. L. Dwyer, *Proc. Combust. Inst.* **1990**, *23*, 179.
- [18] R. L. Vander Wal, A. J. Tomasek, *Combust. Flame* **2004**, *136*, 129.
- [19] R. L. Vander Wal, A. J. Tomasek, T. M. Tichich, *Nano Lett.* **2003**, *3*, 223.
- [20] F. Cataldo, M. A. Pontier-Johnson, *Fullerenes Nanotubes Carbon Nanostruct.* **2002**, *10*, 1.
- [21] F. Banhart, P. M. Ajayan, *Adv. Mater.* **1997**, *9*, 261.
- [22] J. Y. Huang, *Nano Lett.* **2007**, *7*, 2335.
- [23] J. Guo, X. Wang, T. Wang, *J. Appl. Phys.* **2007**, *101*, 063537.
- [24] J. Hou, X. Wang, P. Vellelacheruvu, J. Guo, C. Liu, H. M. Cheng, *J. Appl. Phys.* **2006**, *100*, 124314.
- [25] H. Cui, Y. Sun, G. Z. Yang, J. Chen, D. Jiang, C. X. Wang, *Chem. Commun.* **2009**, *41*, 6243.
- [26] X. D. Wang, J. Zhou, C. S. Lao, J. H. Song, N. S. Xu, Z. L. Wang, *Adv. Mater.* **2007**, *19*, 1627.
- [27] N. S. Liu, G. J. Fang, W. Zeng, H. Long, L. Y. Yuan, X. Z. Zhao, *Appl. Phys. Lett.* **2009**, *95*, 153505.
- [28] R. H. Fowler, L. Nordheim, *Proc. R. Soc. London, Ser. A* **1928**, *119*, 173.
- [29] J. Robertson, *J. Vac. Sci. Technol., B* **1999**, *17*, 659.